MR Imaging with Remote Control: Feasibility Study in Cardiovascular Disease[1]

J. Paul Finn, MD
Roya Saleh, MD
Stefan Thesen, PhD
Stefan G. Ruehm, MD
Margaret H. Lee, MD
John Grinstead, PhD
John S. Child, MD
Gerhard Laub, PhD

The institutional review board approved this HIPAA-compliant study and waived informed consent. The purpose was to retrospectively evaluate remote control magnetic resonance (MR) imaging in complex cardiovascular procedures, whereby operational expertise was made available locally from a remote location. Thirty patients underwent cardiac (12 patients) and/or vascular (30 patients) 1.5-T MR imaging with a remote operator by using a personal computer. All patient studies were compared with 30 control studies obtained with conventional local imaging. Cardiac cine, myocardial delayed enhancement, and MR angiograms were assessed for overall image quality and motion artifact. MR angiograms were evaluated for vascular definition. Image quality was excellent in 90% (38 of 42) of remote images versus 60% (25 of 42) of control group images ($P < .01$). Scores for motion artifact were not significantly different ($P = .11$). Interactive MR imaging was successfully implemented with remote control in complex cardiovascular cases; diagnostic quality of images was superior to that of images obtained locally.

[1] From the Departments of Radiological Sciences (J.P.F., R.S., S.G.R., M.H.L.) and Medicine (J.P.F., J.S.C.), David Geffen School of Medicine, University of California at Los Angeles, Peter V. Ueberroth Bldg, Suite 3371, 10945 Le Conte Ave, Los Angeles, CA 90095-7206; Siemens Medical Solutions, Erlangen, Germany (S.T.); and Siemens Medical Solutions, Los Angeles, Calif (J.G., G.L.). Received November 23, 2005; revision requested January 3, 2006; revision received January 21; accepted February 8; final version accepted April 3. **Address correspondence to** J.P.F. (e-mail: *pfinn@mednet.ucla.edu*).

Cardiovascular magnetic resonance (MR) imaging exemplifies powerful, but operationally complex, technology. Use of MR imaging for functional and anatomic cardiac imaging (1–7), myocardial viability imaging (7–14), and a broad spectrum of angiographic techniques (15–23) has become widespread. Cardiovascular MR imaging procedures, however, differ from more traditional MR applications in several respects. The operator must understand relevant cardiac and vascular anatomy and pathophysiology; prescribe the correct imaging planes; synchronize various data acquisition windows with contrast agent injection schemes; and choose appropriate values for pulse sequence parameters, parallel imaging factors, and spatial and temporal resolution.

In some practices, radiologists are uncomfortable about accepting requests for cardiovascular MR procedures for lack of sufficient on-site technical expertise. In other practices, MR imaging machines are geographically distributed over several facilities such that there are insufficient trained technologists to provide adequate coverage of all systems, and this shortfall results in scheduling challenges that can affect patient care. To address the problem of having several locations for imaging units campus-wide and to make specialist skills available for the benefit of all patients, we developed network connectivity for complex cardiovascular MR imaging.

Thus, the purpose of our study was to retrospectively evaluate remote control MR imaging in complex cardiovascular procedures, whereby operational expertise was made available locally from a remote location.

Advances in Knowledge

- To our knowledge, ours is the first description of clinical MR imaging performed by using remote control.
- Remote control imaging can provide specialist technical support at the imaging unit.
- Specialized cardiovascular studies in adults and children, which might otherwise be impractical, can be performed with remote control MR imaging.

Materials and Methods

During a 6-month period, we performed diagnostic remote control (remote operator has direct interactive control over the machine) cardiac and/or vascular MR imaging in 30 adult and pediatric patients. The study was performed in accordance with a protocol approved by the University of California at Los Angeles institutional review board, and the requirement for informed consent was waived. Our study was Health Insurance Portability and Accountability Act compliant.

Remote Imaging Setup

The remote MR imaging connectivity was implemented with assistance from Siemens Medical Solutions, Erlangen, Germany; however, the non–Siemens Medical Solutions employees had control of information and data that might present a conflict of interest for the employees. For remote imaging, a personal computer running Windows XP operating system (Microsoft, Redmond, Wash) and located 0.5 mile from an inpatient MR imaging unit was used to emulate the local MR imaging console. The remote personal computer used for the current study had a 2-GHz central processing unit, 256-MB random access memory, and a graphics board capable of displaying 1280 × 1024 pixels from the graphical user interface, with a color depth of 32 bits. The remote console was slaved to the local console through virtual network computing (VNC) (24) software, and connectivity was mediated via the institutional intranet with a maximum bandwidth of 1 MB/sec.

Access to the VNC program was password protected so that only a legitimate operator could log on remotely to the MR imaging unit user interface. The monitor and keyboard of the remote console and the MR imaging unit were identical. Prior to logging on, the remote operator (J.P.F.) established audio communication with the local MR imaging technologist with a hands-free phone connection and announced his intention to go online. Once he logged on, the remote operator and local technologist had equal access and priority on the user interface, and all mouse movements made by the remote operator were visible to the local technologist. For our study, once the remote operator logged on, he requested that the local technologist relinquish full control of the MR imaging console, whereas the local technologist controlled all aspects of patient positioning and communication, patient comfort, patient monitoring, and patient safety in the MR imaging environment. During the procedure, continuous audio communication was maintained between both parties via the same hands-free telephone connection.

Because the VNC application reproduces the MR imaging unit console at the remote console and utilizes the central processing unit of the host (MR imaging unit) computer, the remote operator had full interactive control over all functionality of the MR imaging unit, including the graphical user interface and real-time image viewing (Fig 1). For our study, the remote operator performed all aspects of the imaging procedure that did not involve direct communication with the patient or intravenous injection of contrast medium. The types of studies performed are detailed later.

The clinical imaging studies routinely involved breath-hold image acquisition, as well as timed intravenous contrast medium injection. The local tech-

Published online before print
10.1148/radiol.2412051898

Radiology 2006; 241:528–537

Abbreviation:
VNC = virtual network computing

Author contributions:
Guarantor of integrity of entire study, J.P.F.; study concepts/study design or data acquisition or data analysis/interpretation, all authors; manuscript drafting or manuscript revision for important intellectual content, all authors; manuscript final version approval, all authors; literature research, J.P.F., R.S., S.T.; clinical studies, J.P.F., S.G.R., M.H.L.; statistical analysis, R.S.; and manuscript editing, all authors

See Materials and Methods for pertinent disclosures.

nologist was responsible for giving breathing instructions to the patient and controlled the electronic contrast medium injector. In turn, the remote operator controlled the choice of imaging protocol, pulse sequences, image orientation, section thickness and offsets, bandwidth, spatial resolution, field of view, acquisition time, k-space trajectory, and postprocessing options. The procedure time was defined as the time from the acquisition of the first localizer image to completion of the last imaging sequence. Start time and completion time were documented for all studies, as were contrast agent dose and a statement as to which, if any, complications occurred. Once the procedure was completed, the remote operator remained online to complete any postprocessing deemed appropriate and sent the relevant images to the picture archiving and communications system archive. At that point, he logged off and terminated the connection. In the interim, the local technologist escorted the patient from the MR imaging suite.

Figure 1

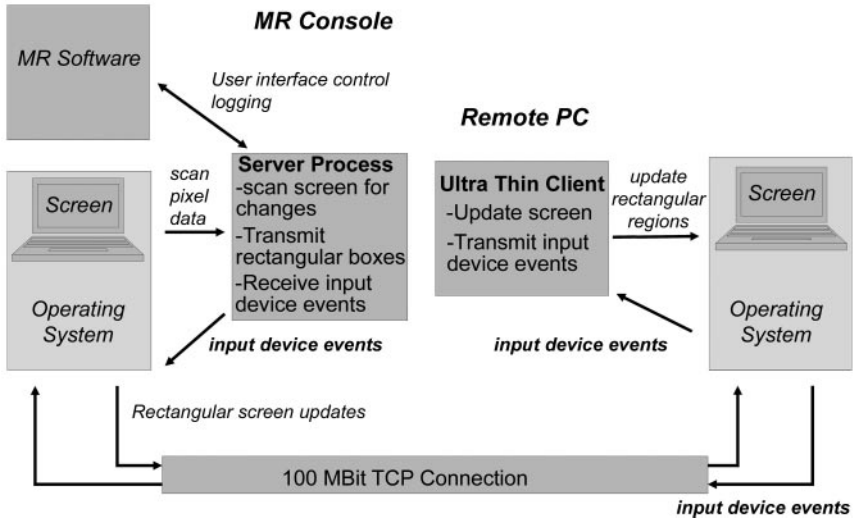

Figure 1: Diagrammatic representation of information flow between remote and local consoles. VNC connectivity between MR imaging unit and remote personal computer *(PC)* was mediated through the University of California at Los Angeles Medical Center local area network. Keyboard inputs at the remote console are transmitted by using a 100-megabit transmission control protocol *(TCP)* connection to the MR imaging operating system, software, and screen. Updates from the MR imaging unit interface (graphics and text) are returned to the remote console in real time by using the same VNC connection.

Patients and Control Subjects

The study subjects comprised a cohort of patients who underwent imaging remotely and a control group of subjects who underwent imaging with local control in the conventional way. The remote imaging and control groups each contained 30 patients who underwent cardiac MR imaging, MR angiography of the chest, or abdominal MR angiography. In the remote imaging group, patients were imaged sequentially between November 2004 and July 2005 by one remote operator (J.P.F., with 15 years of experience), and none were excluded. The 30 control subjects were identified retrospectively so that they were matched to the subjects in the remote imaging group as closely as practical according to age and type of MR imaging study. The inclusion criterion for the control subjects was that each be within 10 years in age of the corresponding patients for adults and within 1 year in age of the corresponding patients for children. Thus, 42 images (12 cardiac MR images, 10 abdominal MR angiograms, and 20 chest MR angio-

Table 1

Reason for Clinical Referral

Reason	Remote Image*	Local Image*
Thorax†		
Cardiac tumor vascular assessment	1	1
Cardiac tumor postsurgical resection assessment	2	1
Assessment of cardiac morphology and function	10	11
Cardiac shunt patency assessment	2	2
Myocardial infarction viability assessment	3	3
Superior vena cava assessment	1	3
Thoracic aorta assessment	4	2
Thoracic vascular assessment	6	9
Abdomen		
Assessment of abdominal aorta and its branches	4	3
Abdominal venous system evaluation	1	3
Inferior vena cava and/or portal vein patency assessment after liver transplantation	2	1
Hepatic tumor vascular assessment	0	1
Vascular assessment before liver transplantation	1	0
Vascular assessment after liver transplantation	1	1
Vascular assessment before renal transplantation	1	0
Renal artery stenosis assessment	2	1
Assessment after bowel transplantation and bleeding	1	1

* Data are numbers of patients.

† In some patients, referrals involved more than one clinical question.

grams) obtained in 30 individuals (16 children and 14 adults) were evaluated in each group. In the remote imaging group (13 female and 17 male patients), the mean age for children was 2.54 years ± 2.0, and the range was 1–7 years; for adults, the mean age was 53.4 years ± 17.1, and the range was 20–81 years. In the control group (14 female and 16 male subjects), the mean age for children was 2.86 years ± 2.0, and the range was 1–8 years; for adults, the mean age was 56.4 years ± 17.4, and the range was 20–89 years. The underlying clinical questions varied (Table 1).

The experience of the local technologist who imaged the control subjects was neither an exclusion nor an inclusion criterion but rather reflected real-world institutional practice and routine technologist scheduling. A subgroup of nine patients from the control group underwent imaging performed by the same operator (J.P.F.) as the one who performed imaging of the patients in the remote imaging group. The remaining 21 patients in the control group were imaged by one of six MR imaging technologists, with an average of 9 years of experience (range, 2–15 years).

Image Acquisition

All subjects in the remote imaging and control groups were imaged with the same machine, which was a four-receiver-channel 1.5-T imaging unit (Magnetom Sonata; Siemens Medical Solutions, Malvern, Pa) with high-performance gradients (maximum gradient strength, 40 mT/m; slew rate, 200 $(mT \cdot m^{-1})$/msec, and there were no changes in hardware or software platforms used in either group. For cardiac MR imaging, electrodes were placed on the anterior chest wall, and continuous electrocardiographic monitoring was employed. The electrocardiographic signal was input to the patient monitoring unit for electrocardiographically gated measurements, as required. In adults, the minimum protocol involved multiplanar breath-hold steady-state free precession cine imaging (2–7) and delayed T1-weighted segmented inversion recovery steady-state free precession for hyperenhancement imaging of myocardial scar (12–14). All MR angiographic studies involved timed contrast agent infusion via an electronic injector (Spectris Solaris; Medrad, Indianola, Pa) and three-dimensional acquisition in multiple phases during suspended respiration (16–21). Timing was based on a prior test injection as previously described (16). In adults, a four-channel body phased-array coil was used for signal reception. In children, depending on their size, an adult head coil, knee coil, or body phased-array coil was employed.

In children of both groups, all MR imaging examinations were performed with a general anesthetic (25–27). After successful stabilization of the patient, the patient was advanced into the bore of the MR imaging unit in the supine position with the appropriate coils in place. Continuous electrocardiographic monitoring, pulse oximetry, and noninvasive blood pressure measurement were performed. All aspects of safety and care of the pediatric patients were supervised by specialist pediatric anesthesiologists. Patient positioning, coil positioning, and setup of the electronic contrast agent injector were supervised by the local MR imaging technologist. The remote operator was involved in prior discussions concerning preparation and setup with the anesthesiologist and local technologist by phone but was not physically present during any aspect of preparation or imaging. For the control group, an experienced radiologist was present routinely during the imaging procedure.

Image Analysis

All images from patients in remote imaging and control groups were evaluated in consensus by two specialist cardiovascular reviewers (M.H.L. and S.G.R., with 5 and 10 years of experience, respectively). The reviewers were blinded to the patient's information, clinical details, and whether the images were acquired by a remote operator or local technologist. Cardiac cine, myocardial delayed enhancement, and MR

Figure 2

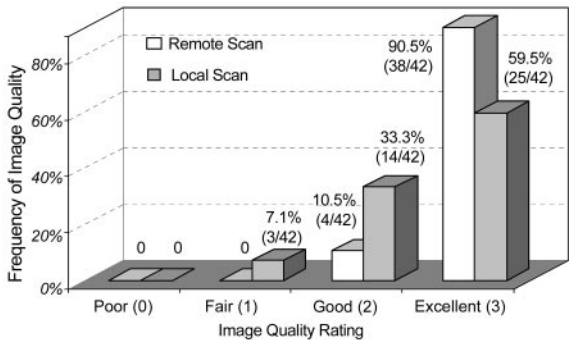

Figure 2: Graph shows frequency of image quality rating for remote and local images in all cardiac and vascular studies. Note the higher percentage of excellent ratings for remote images ($P < .01$). Numbers in parentheses on the x-axis are grades for image quality rating.

Figure 3

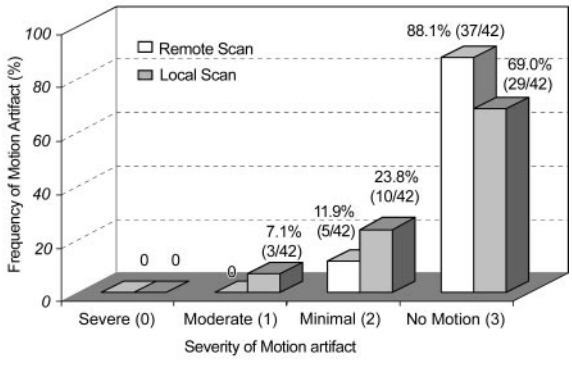

Figure 3: Graph shows frequency of severity of motion artifact rating for remote and local images. There was no statistically significant difference between the groups ($P = .11$). Numbers in parentheses on the x-axis are grades for severity of motion artifact rating.

angiographic images were assessed for overall image quality and motion artifact by using a four-point scoring system that was the same as that for the MR angiographic evaluation.

For qualitative evaluations of all MR angiograms, the reviewers had access to the three-dimensional partition MR angiograms, as well as to full-thickness maximum intensity projections and to multiple overlapping thin maximum intensity projection reconstructions. MR angiograms were assigned scores for overall image quality, motion artifacts, and vessel sharpness.

Subjective criteria for image quality and motion artifact both were defined with a four-point scale grading system. For image quality, the scale was as follows: grade 0, poor nondiagnostic images; grade 1, fair images with reservations about diagnostic content; grade 2, good images with confidence in diagnostic content; and grade 3, excellent images with a very high level of confidence in diagnostic content.

For motion artifact, the scale was as follows: grade 0, severe artifact, which resulted in nondiagnostic images; grade 1, moderate artifact, which degraded diagnostic confidence; grade 2, minimal artifact, which did not interfere with diagnostic confidence; and grade 3, no motion artifact.

Visualization and sharpness of vascular structures were assessed with a four-point scale: grade 0, not seen because of technical factors (motion artifact or poor contrast agent administration timing); grade 1, poorly defined such that stenosis would be difficult to evaluate; grade 2, well defined such that stenosis could be confidently evaluated; and grade 3, excellent definition such that even mild vessel irregularity could be confidently diagnosed.

The following named arteries were evaluated: celiac artery; common, right, and left hepatic arteries; proximal, middle, and distal superior mesenteric arteries; left gastric artery; gastroduodenal artery; and left and right renal arteries. In the chest, up to subsegmental (fourth-order) pulmonary vessel branches were evaluated in the upper and lower lobes of each lung.

Figure 4

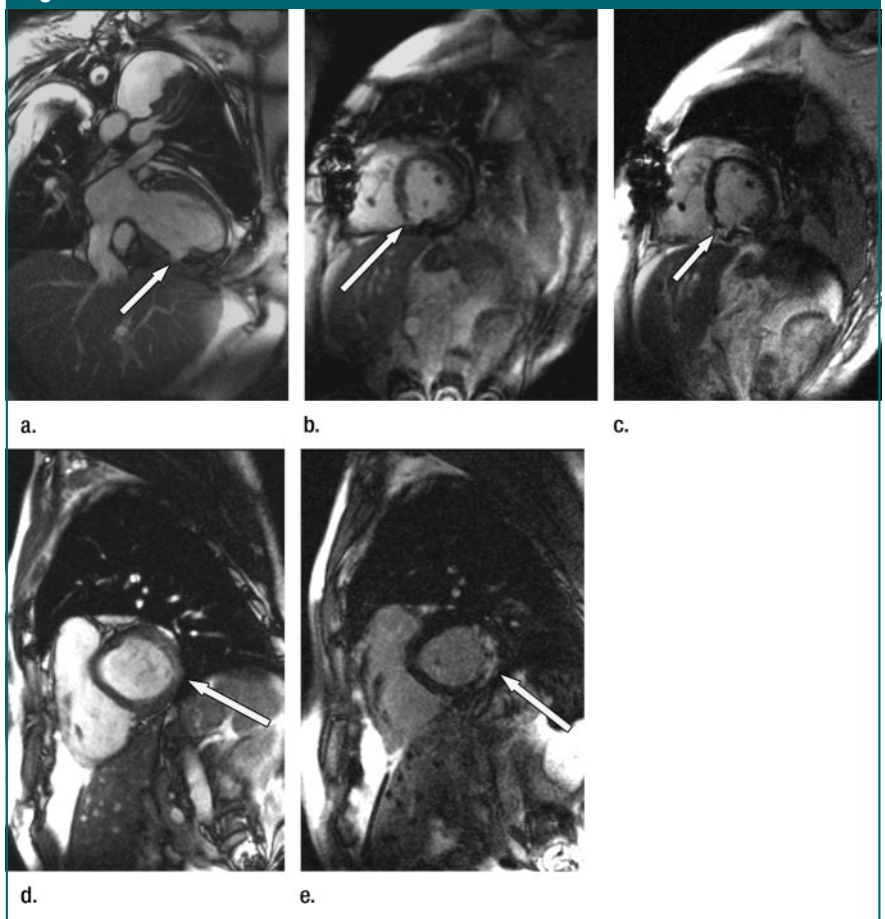

Figure 4: **(a–c)** Immediately postoperative remote cardiac MR images in 70-year-old woman with surgically repaired ventricular septal defect, which occurred as a complication of inferoseptal myocardial infarction (arrow). **(a)** Steady-state free precession cine MR image (repetition time msec/echo time msec, 3.4/1.2; flip angle, 60°) in vertical long-axis view shows focal defect. **(b)** Midchamber short-axis view of same defect in **a** shows that it had been oversewn and no residual interventricular shunt was present. **(c)** Delayed short-axis image (repetition time msec/echo time msec/inversion time msec, twice the R-R interval/4.3/280; flip angle, 30°) shows inferior wall hyperenhancement corresponding to site of transmural myocardial infarction. **(d, e)** Local cardiac MR images in 60-year-old man after ablation therapy for ventricular tachycardia. **(d)** Short-axis cardiac cine image (3.4/1.2; flip angle, 65°) demonstrates hypokinesis of lateral and inferolateral left ventricular wall. Arrow = segment of infarcted myocardium. **(e)** Short-axis delayed hyperenhancement image (twice the R-R interval/4.3/280; flip angle, 30°) shows scar (arrow) of lateral and inferolateral left ventricular myocardium. Both **d** and **e** were obtained by the same operator and have overall image quality comparable to that of **a–c**.

Statistical Analysis

To test the mean difference for imaging duration in both groups, a paired *t* test was used. The Wilcoxon signed rank test was used for comparative analysis of the ordinal data for image quality, motion artifact, and vessel visibility. A paired *t* test was used for comparison of the imaging duration in both groups. Software (SPSS 13.0; SPSS, Chicago, Ill) was used for all statistical evaluations. For all comparisons, $P < .05$ was considered to indicate a statistically significant difference. The mean values of visibility scores are presented to reflect definition of each vessel branch. Power calculations to assess the required sample size could not be performed in advance because no estimate of the standard deviation of the difference between the remote control images and local images was available. After review

of interim data from the first 15 subjects for image quality, however, a power calculation (two-sided paired *t* test) was performed on the basis of the standard deviation estimated from these data. To establish a power of 80% and a level of significance with $\alpha = .05$, a sample size of 30 was estimated in each group. For overall assessment of vessel visibility, a generalized estimating equations model was used with statistical software (SAS 9.0; SAS Institute, Cary, NC).

Results

Imaging Duration

Mean imaging duration for combined cardiac MR imaging and thoracic MR angiography was 53.5 minutes ± 11.1 in the remote imaging group and 53.8 minutes ± 11.6 in the control group ($P = >.99$). Mean imaging duration for abdominal MR angiography was 28.7 minutes ± 7.5 in the remote imaging group and 35.6 minutes ± 11.6 in the control group ($P = .37$).

Image Quality and Motion Artifact Assessment

Image quality was rated excellent in 90% (38 of 42) of remote images and in 60% (25 of 42) of control group images ($P < .01$) (Fig 2). Motion artifact was not assigned scores that were significantly different ($P = .11$) between the two groups (Figs 3–6).

Vascular Segment Assessment

For the MR angiographic analysis, a total of 489 vascular segments were assessed in each group. Vessel sharpness in the thorax and abdomen was rated higher on the remote images, but the difference reached statistical significance only for specific vessel groups (Tables 2, 3; Figs 7, 8). For overall assessment of data in the abdomen and thorax, a generalized estimating equations model was used. With generalized estimating equations, analysis of the thoracic data yielded an overall *P* value of .075, which indicated an overall tendency for better vessel visibility on remote images, but this difference did not reach statistical significance. With generalized estimating equations, analysis of the abdominal data yielded an overall vessel score with a *P* value of .53, which indicated that there was no statistically significant difference in overall visibility assessments in remote and local images.

Discussion

Our results indicate that MR imaging with remote control is entirely feasible and, within the context described, can produce results at least as good as can MR imaging with local control. Because the types of diagnostic studies described are among the most complex currently undertaken (including those in pediatric patients with congenital cardiovascular disorders), it seems reasonable to suggest that the results can be generalized to other types of studies. On average, the diagnostic quality of the remote images was assigned a score that was higher than that for control images, which likely reflected the more varied experience levels among the local technologists compared with the experience level of the remote operator.

In the current implementation of remote imaging, a VNC derivative was used as a starting point. VNC is an open-source platform-independent protocol for controlling a computer from a remote console with a standard transmission control protocol. A transmission control protocol enables two hosts to establish a connection and exchange streams of data. For current purposes, one of these hosts is termed the local console (that of the MR imaging machine), and the other is named the remote console. All keyboard and mouse input events are transmitted from the remote console to the MR imaging console, which is to be controlled. The server sends back updates from the local MR imaging console screen. VNC is a protocol that transmits keyboard and mouse events in one direction (in this case, from the remote console to the local MR imaging console) and allows updating of rectangular sections of the screen on the remote console. The software consists of two main parts. First, a server process runs on the machine to be controlled remotely. This server pro-

Figure 5

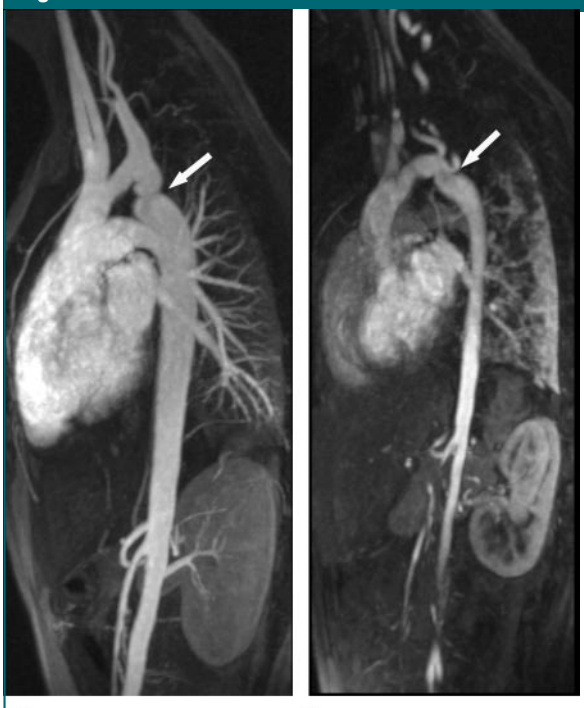

Figure 5: **(a)** Remotely controlled contrast material–enhanced lateral projection MR angiogram (3.1/1.1; flip angle, 25°) in 81-month-old boy with untreated aortic coarctation shows moderate coarctation (arrow) of distal arch. **(b)** Locally controlled contrast-enhanced lateral projection MR angiogram (3.1/1.1; flip angle, 25°) in 68-month-old boy with untreated aortic coarctation (arrow) shows some motion artifact and blurring.

cess scans the local screen for updates on a pixel-by-pixel basis and processes the input device events. On the remote machine, lightweight viewer software for display and collection of the input device events is used. This kind of software is usually called an "ultra-thin client."

Various implementations of VNC available for Windows-based personal computers differ in the mechanisms used to pack the screen updates efficiently. In the current study, so-called ultra-encoding (*http://www.ultravnc.com*) was used. By using this mechanism, high-display performance can be achieved without a compromise of display quality caused by, for example, lossy compression of data. The remote computer for the current study was a 2-year-old personal computer with a 2-GHz central processing unit, 256-MB random access memory, and a graphics board capable of displaying 1280 × 1024 pixels from the graphical user interface, with a color depth of 32 bits. The standard 100-megabit connection used on the institutional medical network was used.

Usually, when remote connections are used in large networks or over a long distance, care has to be taken that the network performance requirements are fulfilled. For the remote connections used between the MR imaging console and the remote personal computer, no encryption was used because the work was performed in a closed, single-institution network. State-of-the-art encryption technology (as in virtual private networks), however, can readily be implemented, thus guaranteeing security for work encompassing more than a single administrative entity. The effect of encryption on software performance remains to be evaluated.

Our motivation for developing the remote imaging tool was to address the very real problem of coordinating complex cardiovascular studies with limited availability of radiologists and technologists. Because of our geographically distributed imaging unit base, and the unpredictable nature of inpatient requests for images, we often have complex studies scheduled in close temporal proximity but in widely separate physical locations. Having the ability to control and monitor several machines from a central hub is a huge advantage in dealing with this type of problem. With the software tools described previously, we were able to image patients by using remote control with no noticeable compromise in performance when com-

Figure 6

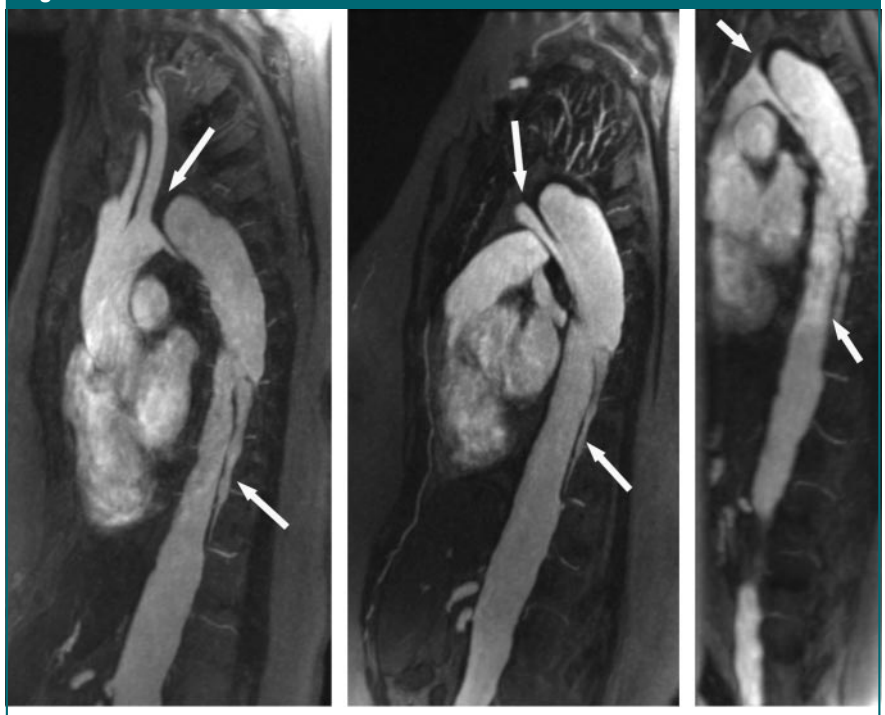

Figure 6: Sagittal images in 33-year-old woman with Marfan syndrome and aortic dissection. The patient underwent surgical intervention (endarterectomy of supraceliac aorta to inframesenteric aorta) 1 year previously and had subsequent short-gut syndrome, paraplegia, and acute renal failure. **(a)** Sagittal projection from remote contrast-enhanced MR angiogram (2.9/0.9; flip angle, 25°) shows complex dissection flap (arrows, also on **b** and **c**) extending from aortic arch to proximal abdomen. **(b)** Follow-up contrast-enhanced MR angiogram (2.9/0.9; flip angle, 25°) obtained locally 3 months later by the same operator shows stable appearance. **(c)** Follow-up contrast-enhanced MR angiogram (2.9/0.9; flip angle, 25°) obtained 6 months later by local technologist with limited experience shows some blurring of dissection flap from motion and limited spatial resolution.

Figure 7

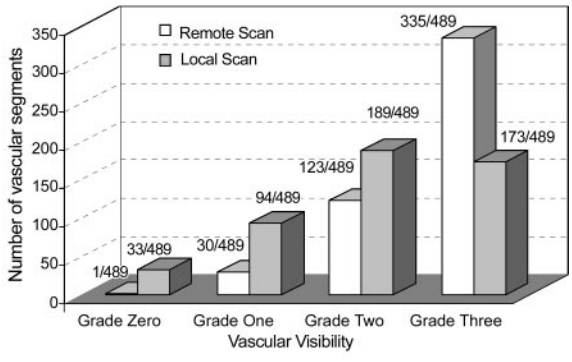

Figure 7: Graph shows number of vessel segments assigned scores for vessel definition on remote and local high-spatial-resolution MR angiograms. Note higher visibility in remote images. These differences were statistically significant for depiction of smaller branch arteries ($P < .05$).

Table 2

Mean Scores for Definition for Chest Vessels

Lung, Lobe, and Branch Order	*P* Value*	Remote Image†	Local Image†
Right lung			
Upper lobe			
Lobar	.06	3 ± 0	2.66 ± 0.48
Sublobar	.06	2.90 ± 0.17	2.52 ± 0.60
Segmental	.01‡	2.61 ± 0.47	1.95 ± 0.80
Subsegmental	.12	1.95 ± 0.54	1.42 ± 0.92
Lower lobe			
Lobar	.03‡	3 ± 0	2.61 ± 0.49
Sublobar	.01‡	2.90 ± 0.17	2.33 ± 0.73
Segmental	.002‡	2.57 ± 0.48	1.80 ± 0.74
Subsegmental	.09	1.85 ± 0.48	1.33 ± 0.91
Left lung			
Upper lobe			
Lobar	.03‡	3 ± 0	2.61 ± 0.49
Sublobar	.02‡	2.85 ± 0.24	2.23 ± 0.83
Segmental	.008‡	2.61 ± 0.47	1.85 ± 0.91
Subsegmental	.07	1.90 ± 0.51	1.33 ± 0.91
Lower lobe			
Lobar	.008‡	3 ± 0	2.52 ± 0.51
Sublobar	.02‡	2.80 ± 0.30	2.23 ± 0.76
Segmental	<.001‡	2.38 ± 0.58	1.47 ± 0.74
Subsegmental	.02‡	1.80 ± 0.61	1.09 ± 0.83

* The *P* values in this study were derived by using actual ordinal scores for every single vessel branch with its comparison group and the Wilcoxon signed rank test.

† Data are the mean ± standard deviation and are presented to demonstrate the visibility definition of each branch.

‡ Value indicates statistically significant difference.

Table 3

Mean Scores for Definition for Abdominal Vessels

Vessel	*P* Value*	Remote Image†	Local Image†
Celiac artery	.3	2.91 ± 0.15	2.58 ± 0.55
Hepatic artery			
Common	.16	2.91 ± 0.15	2.33 ± 0.77
Right	.02‡	2.83 ± 0.27	1.75 ± 0.91
Left	.003‡	2.58 ± 0.48	1.5 ± 0.66
Gastroduodenal artery	.04‡	2.75 ± 0.37	2 ± 0.66
Left gastric artery	.03‡	2.41 ± 0.58	1.58 ± 0.75
Splenic artery	.13	2.90 ± 0.16	2.25 ± 0.75
Superior mesenteric artery			
Proximal	.3	2.91 ± 0.15	2.58 ± 0.55
Middle	.2	2.75 ± 0.37	2.16 ± 0.83
Distal	.17	2.33 ± 0.66	1.83 ± 0.72
Inferior mesenteric artery	.1	2.41 ± 0.58	1.83 ± 0.58
Renal artery			
Right	.24	2.8 ± 0.32	2.45 ± 0.59
Left	.24	2.83 ± 0.27	2.36 ± 0.69

* The *P* values in this study were derived by using actual ordinal scores for every single vessel branch with its comparison group and the Wilcoxon signed rank test.

† Data are the mean ± standard deviation and are presented to demonstrate the visibility definition of each branch.

‡ Value indicates statistically significant difference.

pared with local imaging. There was no detectable latency in response to mouse clicks or alphanumeric entries on the remote console.

To our knowledge, this is the first report of interactive MR imaging with remote control in patients, and the success of this pilot study points to the potential of the method. Successful interactivity with an MR imaging unit requires real-time, but not necessarily high-bandwidth, connectivity. The response to mouse clicks should be near instantaneous, but it is not necessary to transfer large image files in real time. The requirements are somewhat analogous to a long-distance telephone connection, where small packets of information are transferred very quickly and response latency is highly deleterious. Although the performance of the remote imaging tool was adequate in the current study, network speed is dependent on connectivity between specific local and remote consoles, which must be validated on a case-by-case basis. It is reasonable to postulate, however, that physical separation is not a limitation to remote imaging, and long-distance connections can be successfully implemented. In fact, intercontinental remote control of an electron microscope recently has been realized (28), as has real-time ultrasonographic (US) image transfer from as far away as the international space station via a space-to-ground video link (29–30). Several other applications of remote control robotic surgery and US also have been realized (31–33), with bandwidth specifications not dissimilar to those that we describe in the current study.

Besides serving the clinical needs of a single institution, there are several other potential applications for remote imaging technology. A specialized center might support remote sites that lack the personnel with the appropriate background to perform imaging in complex cases, or a center might help train local technologists by having an expert online during a learning phase. The same functionality may allow applications specialists to support remote customer sites and upload and save protocols to a machine without having to visit

the site. Although not addressed in the current study, there is no technical reason why remote control x-ray computed tomography cannot be implemented in a similar way. Remote control imaging might also support mobile units in disaster areas or battle arenas (34).

Another potential application relates to quality control for multicenter clinical trials that involve specialized MR imaging protocols. Although certain field centers may have the appropriate patient cohort for a trial, they may lack the required expertise for specialized MR imaging. In principle, a core MR imaging laboratory could download and fine-tune protocol files and interact remotely with the local technologists during imaging, thus ensuring consistent quality and strict adherence to protocol. The resulting improvement in quality control might be anticipated to have a positive effect on the number of patients necessary to achieve statistical power, with corresponding savings in time and expense for the study sponsor. These applications, however, remain to be established and validated.

Our study had several limitations, which the authors recognize. Ideally, the same patients would be imaged both locally and remotely so that they would serve as their own control subjects. Also, the same operators would image the same subjects locally and remotely. For practical and ethical reasons, however, this condition was not possible. Furthermore, the work described here represents a feasibility study that involved a limited number of patients within a closed institutional network. It cannot, therefore, address the potential effect of more long-range or interinstitutional imaging, other than in a speculative way. Such studies remain to be performed. Nonetheless, the impetus to develop the tools used in the current study was to provide specialist operator availability within a single distributed institutional network, and we believe that we have succeeded in this goal.

In conclusion, interactive MR imaging with remote control is feasible in complex cardiovascular cases, and the diagnostic quality of the images was at least as good as that obtained with MR imaging with local control. It seems likely that, in time, such functionality may evolve to provide online support on a more widespread basis and to help disseminate advanced imaging techniques, supervision, and training to locations where they are most needed.

Figure 8

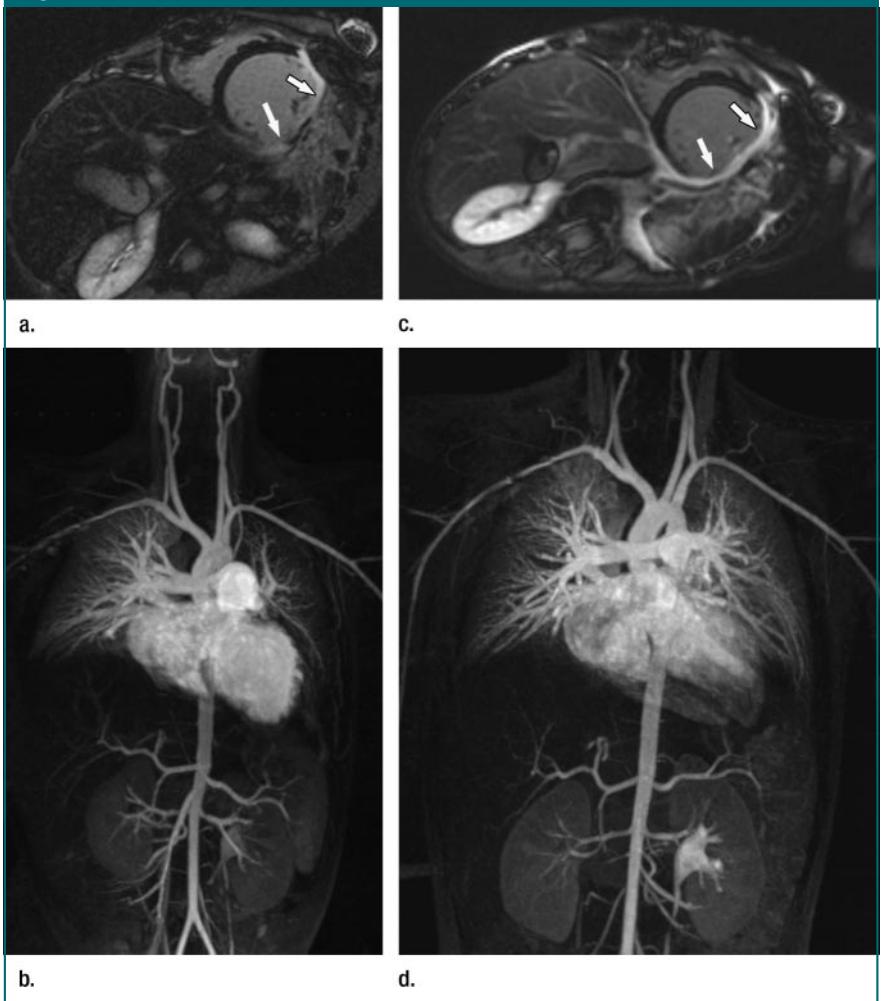

Figure 8: High-grade sarcoma of the myocardium involving the circumflex coronary artery in 5-year-old girl in whom surgical resection was complicated by myocardial infarction. **(a)** Remote delayed hyperenhancement short-axis MR image (twice the R-R interval/1.3/200; flip angle, 50°) of myocardium obtained within 1 month of resection. Extensive transmural hyperenhancement (arrows) is present in lateral and inferolateral left ventricular wall and is consistent with infarction in circumflex coronary artery distribution. **(b)** Remote coronal contrast-enhanced MR angiogram (3/1.1; flip angle, 25°) obtained at same time as **a**. **(c)** Local delayed hyperenhancement short-axis MR image (twice the R-R interval/1.3/220; flip angle, 50°) of myocardium obtained 8 months after resection. Extensive transmural hyperenhancement (arrows) is present in lateral and inferolateral left ventricular wall. **(d)** Coronal contrast-enhanced MR angiogram (2.8/1.0; flip angle, 20°) obtained at same time as **c**. Both images were assigned scores that indicated they were highly diagnostic, with excellent definition of vascular anatomy.

Acknowledgment: Our special thanks to James Sayre, PhD, University of California at Los Angeles, for his assistance with statistical analysis.

References

1. Lorenz CH, Walker ES, Morgan VL, Klein SS, Graham TP Jr. Normal human right and left ventricular mass, systolic function, and gender differences by cine magnetic resonance imaging. J Cardiovasc Magn Reson 1999;1:7–21.
2. Carr JC, Simonetti O, Bundy J, Li D, Pereles

S, Finn JP. Cine MR angiography of the heart with segmented true fast imaging with steady-state precession. Radiology 2001; 219:828–834.

3. Bellenger NG, Gatehouse PD, Rajappan K, Keegan J, Firmin DN, Pennell DJ. Left ventricular quantification in heart failure by cardiovascular MR using prospective respiratory navigator gating: comparison with breath-hold acquisition. J Magn Reson Imaging 2000;11:411–417.
4. Fieno DS, Jaffe WC, Simonetti OP, Judd RM, Finn JP. TrueFISP: assessment of accuracy for measurement of left ventricular mass in an animal model. J Magn Reson Imaging 2002;15:526–531.
5. Kacere RD, Pereyra M, Nemeth MA, Muthupillai R, Flamm SD. Quantitative assessment of left ventricular function: steady-state free precession MR imaging with or without sensitivity encoding. Radiology 2005;235(3):1031–1035.
6. Bellenger NG, Burgess MI, Ray SG, et al. Comparison of left ventricular ejection fraction and volumes in heart failure by echocardiography, radionuclide ventriculography and cardiovascular magnetic resonance: are they interchangeable? Eur Heart J 2000;21: 1387–1396.
7. Miller S, Simonetti OP, Carr J, Kramer U, Finn JP. MR imaging of the heart with cine true fast imaging with steady-state precession: influence of spatial and temporal resolutions on left ventricular functional parameters. Radiology 2002;223:263–269.
8. Kim RJ, Fieno DS, Parrish TB, et al. Relationship of MRI delayed contrast enhancement to irreversible injury, infarct age, and contractile function. Circulation 1999;100: 1992–2002.
9. Simonetti OP, Kim RJ, Fieno DS, et al. An improved MR imaging technique for the visualization of myocardial infarction. Radiology 2001;218:215–223.
10. Kim RJ, Wu E, Rafael A, et al. The use of contrast-enhanced magnetic resonance imaging to identify reversible myocardial dysfunction. N Engl J Med 2000;343:1445–1453.
11. Perin EC, Silva GV, Sarmento-Leite R, et al. Assessing myocardial viability and infarct transmurality with left ventricular electromechanical mapping in patients with stable coronary artery disease: validation by delayed-enhancement magnetic resonance imaging. Circulation 2002;106(8):957–961.
12. Haase J, Bayar R, Hackenbroch M, et al. Relationship between size of myocardial infarctions assessed by delayed contrast-enhanced MRI after primary PCI, biochemical markers, and time to intervention. J Interv Cardiol 2004;17:367–373.
13. Hedstrom E, Palmer J, Ugander M, Arheden H. Myocardial SPECT perfusion defect size compared to infarct size by delayed gadolinium-enhanced magnetic resonance imaging in patients with acute or chronic infarction. Clin Physiol Funct Imaging 2004;24:380–386.
14. Lund GK, Stork A, Saeed M, et al. Acute myocardial infarction: evaluation with first-pass enhancement and delayed enhancement MR imaging compared with 201Tl SPECT imaging. Radiology 2004;232:49–57.
15. Prince MR, Narasimham DL, Stanley JC, et al. Breath-hold gadolinium-enhanced MR angiography of the abdominal aorta and its major branches. Radiology 1995;197:785–792.
16. Earls JP, Rofsky NM, DeCorato DR, Krinsky GA, Weinreb JC. Breath-hold single-dose gadolinium-enhanced three-dimensional MR aortography: usefulness of a timing examination and MR power injector. Radiology 1996; 201:705–710.
17. Wilman AH, Riederer SJ, King BF, Debbins JP, Rossman PJ, Ehman RL. Fluoroscopically triggered contrast-enhanced three-dimensional MR angiography with elliptical centric view order: application to the renal arteries. Radiology 1997;205:137–146.
18. Kreitner KF, Kunz RP, Kalden P, et al. Contrast-enhanced three-dimensional MR angiography of the thoracic aorta: experiences after 118 examinations with a standard dose contrast administration and different injection protocols. Eur Radiol 2001;11:1355–1363.
19. Finn JP, Baskaran V, Carr JC, et al. Thorax: low-dose contrast-enhanced three-dimensional MR angiography with subsecond temporal resolution—initial results. Radiology 2002;224:896–904.
20. Kramer H, Schoenberg SO, Nikolaou K, et al. Cardiovascular screening with parallel imaging techniques and a whole-body MR imager. Radiology 2005;236:300–310.
21. Nael K, Laub G, Finn JP. Three-dimensional contrast-enhanced MR angiography of the thoraco-abdominal vessels. Magn Reson Imaging Clin N Am 2005;13:359–380.
22. Fain SB, Browning FJ, Polzin JA, et al. Floating table isotropic projection (FLIPR) acquisition: a time-resolved 3D method for extended field-of-view MRI during continuous table motion. Magn Reson Med 2004;52(5):1093–1102.
23. Wieben O, Grist TM, Hany TF, et al. Time-resolved 3D MR angiography of the abdomen with a real-time system. Magn Reson Med 2004;52(4):921–926.
24. Richardson T, Stafford-Fraser Q, Wood KR, Hopper A. Virtual network computing. IEEE Internet Comput 1998;2(1):33–38.
25. Holmqvist C, Larsson EM, Stahlberg F, Laurin S. Contrast-enhanced thoracic 3D-MR angiography in infants and children. Acta Radiol 2001;42:50–58.
26. Tsai-Goodman B, Geva T, Odegard KC, Sena LM, Powell AJ. Clinical role, accuracy, and technical aspects of cardiovascular magnetic resonance imaging in infants. Am J Cardiol 2004;94:69–74.
27. Odegard KC, DiNardo JA, Tsai-Goodman B, Powell AJ, Geva T, Laussen PC. Anaesthesia considerations for cardiac MRI in infants and small children. Paediatr Anaesth 2004;14: 471–476.
28. Yamada A, Hirahara O, Tsuchida T, Sugano N, Date M. A practical method for the remote control of the scanning electron microscope. J Electron Microsc (Tokyo) 2003;52: 101–109.
29. Sargsyan AE, Hamilton DR, Jones JA, et al. FAST at MACH 20: clinical ultrasound aboard the International Space Station. J Trauma 2005;58:35–39.
30. Fincke EM, Padalka G, Lee D, et al. Evaluation of shoulder integrity in space: first report of musculoskeletal US on the International Space Station. Radiology 2005;234: 319–322.
31. Costello AJ, Haxhimolla H, Crowe H, Peters JS. Installation of telerobotic surgery and initial experience with telerobotic radical prostatectomy. BJU Int 2005;96:34–38.
32. den Hartog FT, Schmidt JR, de Vries A. Personal networks enabling remote assistance for medical emergency teams. Stud Health Technol Inform 2005;114:221–229.
33. Delgorge C, Courreges F, Al Bassit L, et al. A tele-operated mobile ultrasound scanner using a light-weight robot. IEEE Trans Inf Technol Biomed 2005;9:50–58.
34. Benner T, Schachinger U, Nerlich M. Telemedicine in trauma and disasters—from war to earthquake: are we ready? Stud Health Technol Inform 2004;104:106–115.